Synthesis and Characterization of Mesostructured Tin Oxide with Crystalline Walls

Limin Qi,* Jiming Ma, Humin Cheng, and Zhenguo Zhao

Department of Chemistry, Peking University, Beijing 100871, China

Received September 30, 1997. In Final Form: December 16, 1997

Introduction

Shortly after the original synthesis of silica-based mesoporous molecular materials (MCM-41) with uniformly sized pores,[1,2] the supramolecular templating approach was extended to the synthesis of non-siliceous mesoporous materials based on both transition and main-group metal oxides because of their potential application as solid electrolyte devices, high surface area catalysts, and sorbents, as well as in host−guest chemistry.[3,4] The mesostructured materials of the oxides of W, Sb, and Pb are among the first reported examples of hexagonal mesoporous phases based on metal oxides.[5] Subsequently, three-dimensional mesostructures based on a variety of metal oxides such as the oxides of Ti,[6,7] Zr,[8−10] Hf,[11] V,[12,13] Nb,[14] Ta,[15] and Al[16,17] were synthesized via various templating routes. The obtained mesoporous metal oxide materials usually consist of amorphous walls, although structurally ordered walls can form in certain cases such as the case of ZrO_2.[10] It has been pointed out that since many applications require crystalline materials of specific crystalline structure, it would be advantageous to synthesize mesoporous materials with desired crystalline frameworks.[18,19] Recently, hexagonal mesoporous manganese oxide with walls composed of microcrystallites of dense phases of Mn_2O_3 and Mn_3O_4 has been synthesized and characterized as mixed-valent semiconducting catalysts.[20] It is worthwhile to explore the synthesis of mesostructured materials with crystalline walls based on other metal oxides by means of supramolecular templating.

Tin oxide is a kind of wide energy gap semiconductor and finds many technological applications such as catalysts for oxidation of organics, solid-state gas sensors, and optical electronic devices.[21−23] The success in many of these applications relies on crystalline SnO_2 with a uniform nanosize pore structure. Thus, synthesis of mesoporous SnO_2 with crystalline walls would be of industrial interest. Recently, a mesoporous phase based on SnO_2 has been successfully synthesized by using an anionic surfactant aerosol OT (AOT).[7] However, the obtained mesoporous SnO_2 has not been shown to consist of crystalline walls. Here, we report on the synthesis of mesostructured tin oxide with walls composed of nanocrystalline SnO_2 with the tetragonal cassiterite structure. High-resolution transmission electron microscopy (HR-TEM) was used to directly examine the microstructure of the mesophase with crystalline walls for the first time.

Experimental Section

An anionic surfactant sodium dodecyl sulfonate ($C_{12}S$) was employed as a template for the synthesis of mesostructured SnO_2 with crystalline walls. In a typical synthesis, $C_{12}S$ (1.36 g, 5 mmol) was dissolved in water (100 mL) at 40 °C and then 5 mL of 1 M aqueous $SnCl_4$ solution was added to the $C_{12}S$ solution with stirring, resulting in a milk white suspension. After 5 min of stirring, the mixture was aged for 24 h at room temperature and the suspension settled slowly. The resulting solid white product was recovered by centrifugation, washed with water and acetone successively, and dried at 80 °C for 1 day. The calcination was carried out by heating in air at 400 °C for 2 h with a heating rate of 2 K min^{-1}. For comparison purposes, nanocrystalline SnO_2 without mesostructure was synthesized by adding 5 mL of 1 M aqueous $SnCl_4$ solution to a solution of Na_2SO_4 (0.71 g, 5 mmol) in water (100 mL) with stirring, which caused the immediate precipitation of a white solid. The resulting solid was aged, recovered, washed, and dried in an identical manner.

Powder X-ray diffraction (XRD) patterns in the 2θ range of 1.4−60° were recorded on a Rigaku Dmax-2000 diffractometer using Cu Kα radiation. Conventional transmission electron microscopy (TEM) micrographs were obtained on a JEOL 200CX microscope operated at 200 kV, and HRTEM images were taken with a Hitachi H-9000HAR microscope operated at 300 kV. Samples for TEM and HRTEM were prepared by extensive grinding, sonication in ethanol, and suspension on Formvar-covered and holy carbon-coated copper grids, respectively. Infrared (IR) spectra were obtained with a Nicolet 7199B FTIR spectrometer in KBr medium. Thermogravimetric analysis (TGA) was conducted on a LCT-1 type thermoanalyzer in air.

Results and Discussion

As shown in Figure 1A, the XRD pattern of the SnO_2 material obtained in the presence of Na_2SO_4 shows only a broad shoulder at low angles; however, three broad peaks

(1) Kresge, C. T.; Leonowicz, M. E.; Roth, W. J.; Vartuli, J. C.; Beck, J. S. *Nature* **1992**, *359*, 710.
(2) Beck, J. S.; Vartuli, J. C.; Roth, W. J.; Leonowicz, M. E.; Kresge, C. T.; Schmitt, K. D.; Chu, C. T.-W.; Olson, D. H.; Sheppard, E. W.; McCullen, S. B.; Higgins, J. B.; Schlenker, J. L. *J. Am. Chem. Soc.* **1992**, *114*, 10834.
(3) Huo, Q.; Margolese, D. I.; Ciesla, U.; Feng, P.; Gier, T. E.; Sieger, P.; Leon, R.; Petroff, P. M.; Schuth, F.; Stucky, G. D. *Nature* **1994**, *368*, 317.
(4) Ciesla, U.; Demuth, D.; Leon, R.; Petroff, P.; Stucky, G.; Unger, K.; Schuth, F. *J. Chem. Soc., Chem. Commun.* **1994**, 1387.
(5) Huo, Q.; Margolese, D. I.; Ciesla, U.; Demuth, D. G.; Feng, P.; Gier, T. E.; Sieger, P.; Firouzi, A.; Chmelka, B. F.; Schuth, F.; Stucky, G. D. *Chem. Mater.* **1994**, *6*, 1176.
(6) Antonelli, D. M.; Ying, J. Y. *Angew. Chem., Int. Ed. Engl.* **1995**, *34*, 2014.
(7) Ulagappan, N.; Rao, C. N. R. *Chem. Commun.* **1996**, 1685.
(8) Ciesla, U.; Schacht, S.; Stucky, G. D.; Unger, K. K.; Schuth, F. *Angew. Chem., Int. Ed. Engl.* **1996**, *35*, 541.
(9) Kim, A.; Bruinsma, P.; Chen, Y.; Wang, L.-Q.; Liu. J. *Chem. Commun.* **1997**, 161.
(10) Pacheco, G.; Zhao, E.; Garcia, A.; Sklyarov, A.; Fripiat, J. J. *Chem. Commun.* **1997**, 491.
(11) Liu, P.; Liu, J.; Sayari, A. *Chem. Commun.* **1997**, 577.
(12) Abe, T.; Taguchi, A.; Iwamoto, M. *Chem. Mater.* **1995**, *7*, 1429.
(13) Luca, V.; MacLachlan, D. J.; Hook, J. M.; Withers, R. *Chem. Mater.* **1995**, *7*, 2220.
(14) Antonelli, D. M.; Ying, J. Y. *Angew. Chem., Int. Ed. Engl.* **1996**, *35*, 426.
(15) Antonelli, D. M.; Ying, J. Y. *Chem. Mater.* **1996**, *8*, 874.
(16) Bagshaw, S. A.; Pinnavaia, T. J. *Angew. Chem., Int. Ed. Engl.* **1996**, *35*, 1102.
(17) Vaudry, F.; Khodabandeh, S.; Davis, M. E. *Chem. Mater.* **1996**, *8*, 1451.
(18) Liu. J.; Kim, A. Y.; Wang, L. Q.; Palmer, B. J.; Chen, Y. L.; Bruinsma, P.; Bunker, B. C.; Exarhos, G. J.; Graff, G. L.; Rieke, P. C.; Fryxell, G. E.; Virden, J. W.; Tarasevich, B. J.; Chick, L. A. *Adv. Colloid Interface Sci.* **1996**, *69*, 131.
(19) Raman, N. K.; Anderson, M. T.; Brinker, C. J. *Chem. Mater.* **1996**, *8*, 1682.
(20) Tian, Z.-R.; Tong, W.; Wang, J.-Y.; Duan, N.-G.; Krishnan, V. V.; Suib, S. L. *Science* **1997**, *276*, 926.
(21) Wang, D.; Wen, S.; Chen, J.; Zhang, S.; Li, F. *Phys. Rev. B* **1994**, *49*, 11282.
(22) Dieguez, A.; Romano-Rodriguez, A.; Morante, J. R.; Weimar, U.; Schweizer-Berberich, M.; Gopel, W. *Sens. Actuators, B* **1996**, *31*, 1.
(23) Wu, N.-L.; Wu, L.-F.; Yang, Y.-C.; Huang, S.-J. *J. Mater. Res.* **1996**, *11*, 813.

S0743-7463(97)01077-9 CCC: $15.00
Published on Web 03/31/1998

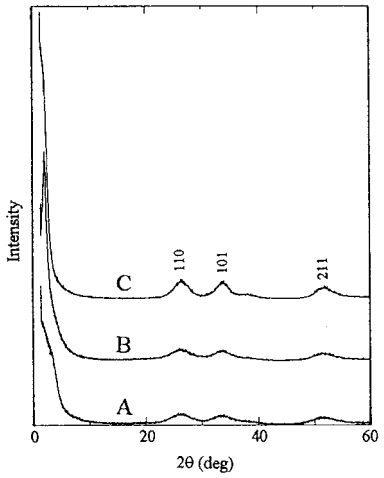

Figure 1. XRD patterns of (A) SnO_2 obtained in the presence of Na_2SO_4, (B) as-synthesized $SnO_2-C_{12}S$, and (C) $SnO_2-C_{12}S$ calcined at 400 °C. The medium-angle patterns are assigned and indexed to the cassiterite structure of SnO_2.

at medium angles are apparent and are assignable to the tetragonal cassiterite structure of SnO_2. According to the Scherrer formula, an average SnO_2 crystallite size of about 1.8 nm in the (110) direction was derived from the half-height breadth of the (110) peak.[21] It is worth noting that the current synthesis of nanocrystalline SnO_2 from $SnCl_4$ usually introduces ammonium hydroxide into the acid salt solution to induce condensation producing oxyhydroxide or oxide precipitates,[21,22] whereas the spontaneous solution−sol−gel transition for pure aqueous $SnCl_4$ solution is very slow.[23] In the present case, sulfate ions seem to act as a precipitation reagent to induce condensation, indicating that sulfate ions and the like, such as sulfonate ions as in the case of $C_{12}S$, may have certain inherent interaction with the Sn(IV) cationic species in the acid solution.

The XRD pattern of the as-synthesized solid product obtained using $C_{12}S$ instead of Na_2SO_4 is shown in Figure 1B. An intense peak at a low angle corresponding to a *d* spacing of 4.1 nm is present, which is relatively broad in view of the wide 2θ range of the figure, and is characteristic of a mesophase with a pore system lacking long-range order. Analogous single peak patterns corresponding to large *d* spacings have been observed for disordered mesoporous silica,[24,25] alumina,[16,17] and zirconia.[10] In addition to the intense peak at large *d* spacing, the three broad peaks assignable to cassiterite are still present, and the intensities and breadths of these peaks are almost identical to those of the peaks in Figure 1A. This indicates that the mesostructured SnO_2 consists of crystalline walls, the average thickness of which is close to 1.8 nm. However, the possibility that the product is a phase mixture of cassiterite and mesostructured amorphous tin oxide cannot be excluded from this XRD pattern. The IR spectrum of the as-synthesized mesophase shows the known features of $C_{12}S$, confirming the presence of the surfactant in the pores. A surfactant content of more than 15 wt % is revealed by the corresponding TGA result. After calcination at 400 °C, most organics are removed as proved by the TGA and IR results for the calcined sample. However, collapse of the mesostructure occurs during calcination, which has been suggested by the disappearance of the large *d* spacing peak in the XRD pattern of the calcined $SnO_2-C_{12}S$ (Figure 1C). It has also been shown that the average crystallite size has grown to about 2.7 nm upon calcination.

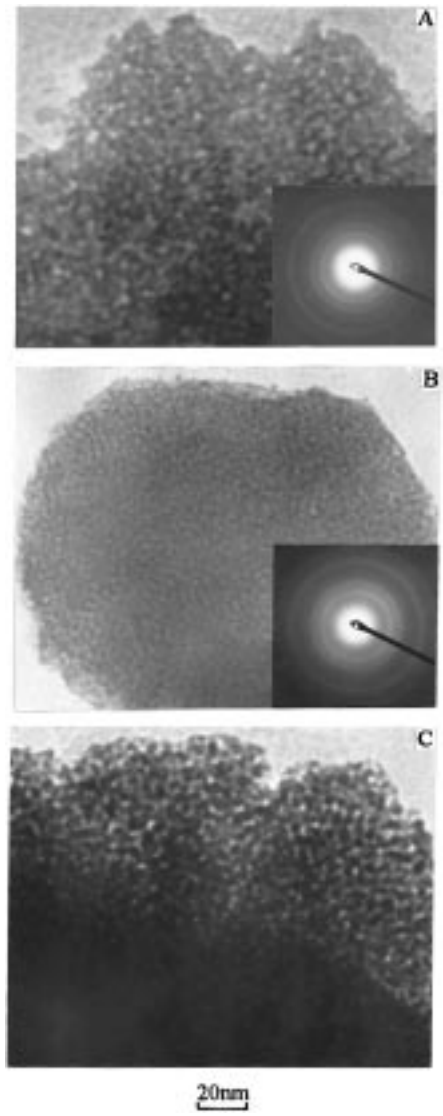

Figure 2. TEM micrographs of (A) SnO_2 obtained in the presence of Na_2SO_4, (B) as-synthesized $SnO_2-C_{12}S$, and (C) $SnO_2-C_{12}S$ calcined at 400 °C. Insets show corresponding electron diffraction patterns.

A representative TEM micrograph of the SnO_2 synthesized without the surfactant is shown in Figure 2A, which reveals the presence of many irregularly sized nanopores. This irregular pore system may bring about a certain degree of short-range structural order and result in the presence of a broad shoulder at low angles in the XRD pattern shown in Figure 1A. The corresponding electron diffraction pattern shows that the three relatively broad fringe patterns with spacings of 0.33, 0.26, and 0.17 nm are consistent with the cassiterite structure SnO_2 (110), (101), (211) spacings. This result reveals that the random network surrounding the irregularly sized holes consists of SnO_2 nanocrystals.

In contrast to the irregularly sized pores in the SnO_2 synthesized without the surfactant, the SnO_2 synthesized in the presence of $C_{12}S$ shows uniformly sized pores (Figure 2B). The wall thickness as well as the pore size is measured to be approximately 2 nm, a value in good agreement with the thickness indicated by the average crystalline size. It can also be seen that the pore structure has no long-range order, which is consistent with the XRD

(24) Tanev, P. T.; Pinnavaia, T. J. *Science* **1995**, *267*, 865.
(25) Bagshaw, S. A.; Prouzet, E.; Pinnavaia, T. J. *Science* **1995**, *269*, 1242.

result. It is noteworthy that a short-range structural order with uniform pore sizes leads to an intense XRD peak at low angles, while a much lower short-range structural order resulting from irregular pore sizes only leads to a broad XRD shoulder at low angles. The electron diffraction pattern corresponding to the $SnO_2-C_{12}S$ mesophase shown in Figure 2B appears to be almost identical to that corresponding to the SnO_2 synthesized without the surfactant. This result proves that the obtained mesostructured SnO_2 consists of nanocrystalline cassiterite, which forms crystalline walls, instead of amorphous tin oxide. Although it still cannot be concluded that the walls are completely composed of crystalline SnO_2, the possibility of the presence of amorphous SnO_2 seems to be rather low since the SnO_2 crystal formation under the present condition occurs readily. Furthermore, the fact that the intensities of the corresponding XRD peaks assignable to cassiterite are almost identical to those corresponding to the SnO_2 obtained without the template strongly indicates that the formation of the $SnO_2-C_{12}S$ mesophase has not impeded the crystal formation of SnO_2.

As shown in Figure 2C, the calcined $SnO_2-C_{12}S$ is composed of grains and holes, which are very irregular in size. The grain sizes of about 2−5 nm are considerably larger than the wall thickness of the as-synthesized $SnO_2-C_{12}S$, which indicates a crystalline size increase upon calcination, confirming the corresponding XRD result. It has been reported that the crystalline size of nanocrystalline SnO_2 readily increases upon calcination even at annealing temperatures lower than 400 °C.[21] This may contribute to the collapse of the SnO_2 mesostructure upon surfactant removal during calcination. It appears that although the SnO_2 crystal formation at room temperature does not become considerable obstacles in obtaining mesostructured SnO_2, the SnO_2 crystal growth upon calcination does become remarkable obstacles in obtaining stable mesoporous SnO_2. Thus, surfactant removal by methods other than calcination seems more promising, and such efforts are currently in progress.

Further information about the microstructure of the as-synthesized $SnO_2-C_{12}S$ mesophase is provided by HRTEM investigation. As shown in Figure 3A, many crystals ranging in width from less than 2 to about 3 nm show clear tetragonal SnO_2 lattice fringes. These nanocrystals connect each other to form crystalline walls, in which are many pores filled with amorphous material probably corresponding to the surfactant. However, due to the random ordering of the pores and the overlapping of the nanocrystalline walls, it is extremely difficult to see evenly distributed, uniformly sized pores in HRTEM images even though different focus planes are used. Figure 3B presents an enlarged HRTEM image showing

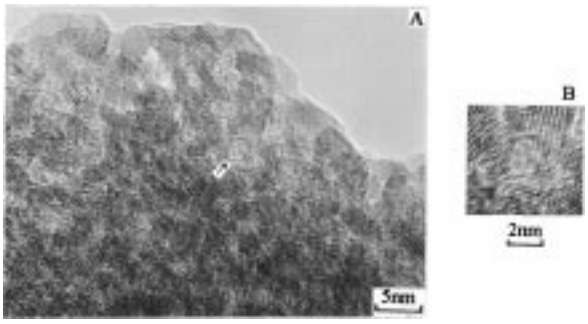

Figure 3. (A) HRTEM image of as synthesized $SnO_2-C_{12}S$. (B) magnification of a single pore in A.

a single pore about 2 nm in size, which is indicated by the arrow in Figure 3A. The pore apparently filled with amorphous surfactant is surrounded by a crystalline wall consisting of tetragonal SnO_2 nanocrystals. The nanocrystals connected to form the wall are randomly directed with many crystal defects present in the interface between them. The interface between the nanocrystalline wall and the enclosed amorphous area shows also disordered structure. Our HRTEM observations of the SnO_2 synthesized in the presence of Na_2SO_4 have shown that there are many nanocrystals connected to form a random network and the hole sizes are rather irregular, which is reminiscent of the "nanosponge structure" in the dry gel SnO_2.[21] This comparison suggests that the major difference in the microstructures between the SnO_2 synthesized with and without the surfactant lies in the uniformity of the pore sizes. These results indicate that HRTEM is a useful method for directly examining the microstructure of mesostructured materials with crystalline walls. However, the use of HRTEM to study the wall structures and wall thickness has its limitation considering that the apparent contrast is sensitive to the photographic conditions and the electron beam could induce possible crystal grain growth.

In conclusion, a mesostructured phase based on SnO_2, which has randomly ordered pores and crystalline walls consisting of tetragonal SnO_2 nanocrystals, can be synthesized by using an anionic surfactant as template. HRTEM has been used to provide direct information about the microstructure of the mesostructured phase with crystalline walls for the first time.

Acknowledgment. The support from the National Natural Science Foundation of China (Project 29733110) and the State Key Program Foundation of China is gratefully acknowledged.

LA971077C